JOURNAL OF VIROLOGY, May 1999, p. 3789–3799 Vol. 73, No. 5
0022-538X/99/$04.00+0

Modulation of Phosphate Uptake and Amphotropic Murine Leukemia Virus Entry by Posttranslational Modifications of PIT-2

PIERRE RODRIGUES AND JEAN MICHEL HEARD*

Laboratoire Rétrovirus et Transfert Génétique, CNRS URA 1157, Institut Pasteur, 75724 Paris, France

Received 4 September 1998/Accepted 19 January 1999

PIT-2 is a type III sodium phosphate cotransporter and the receptor for amphotropic murine leukemia viruses. We have investigated the expression and the functions of a tagged version of PIT-2 in CHO cells. PIT-2 remained equally abundant at the cell surface within 6 h following variation of the phosphate supply. In contrast, the efficiency of phosphate uptake and retrovirus entry was inversely related to the extracellular phosphate concentration, indicating that PIT-2 activities are modulated by posttranslational modifications of cell surface molecules induced by phosphate. Conformational changes of PIT-2 contribute to both activities, as shown by the inhibitory effect of sulfhydryl reagents known as inhibitors of type II cotransporters. A physical association of PIT-2 with actin was demonstrated. Modifications of the actin network were induced by variations of the concentrations of extracellular phosphate, cytochalasin D, or lysophosphatidic acid. They revealed that the formation of actin stress fibers determines the cell surface distribution of PIT-2, the internalization of the receptor in response to virus binding, and the capacity to process retrovirus entry. Thus, the presence of PIT-2 at the cell surface is not sufficient to ensure phosphate transport and susceptibility to amphotropic retrovirus infection. Further activation of cell surface PIT-2 molecules is required for these functions.

Three families of sodium-dependent phosphate (NaP_i) cotransporters have been identified in eukaryotes. The type I NaP_i cotransporter (NaP_i-1) is expressed mostly in the kidneys and liver (15). Type II NaP_i cotransporters (NaP_i-2 to NaP_i-7) are present in the brush border membrane of renal proximal tubules and intestine microvilli (21). Type III NaP_i cotransporters include the mammalian PIT-1 and PIT-2 cotransporters and the Pho-4 protein of the filamentous fungus *Neurospora crassa*. PIT-1 and PIT-2 are widely expressed in mammalian tissues (2). No significant homology has been found for type I and type II NaP_i cotransporters, but structural similarities may exist. Predicted amino acid sequences indicate 10 potential transmembrane domains and a large hydrophilic loop near the center of the molecule. These molecules were originally identified as cell surface receptors for oncoretroviruses (20). PIT-2 serves as a receptor for murine leukemia viruses (MLV) coated with the amphotropic envelope (amphotropic MLV [A-MLV]). Although A-MLV-derived vectors are now broadly used for gene therapy purposes, very little is known about the biology of their receptor.

Retrovirus entry is initiated by the binding of envelope glycoproteins to cell surface receptors. Subsequent refolding of the heterotrimeric envelope glycoproteins reveals fusogenic epitopes. Following fusion of the viral envelope with the plasma membrane, the viral core is released in the cytosol. The fusion reaction may require a low-pH environment, as for ecotropic MLV and MLV pseudotypes bearing the vesicular stomatitis virus envelope glycoprotein (VSV-G), or may be independent of pH, as for A-MLV. With regard to pH dependence, it is thought that fusion occurs in endosomal vesicles for ecotropic and VSV-G envelopes, whereas it could take place at the cell surface for amphotropic viruses (30). However, how receptors contribute to the entry process is not understood.

The regulation of the transmembrane transport of inorganic phosphate (P_i) is crucial for the maintenance of the intracellular P_i pool and for the homeostatic control of the phosphate concentration. Phosphate uptake is adjusted in response to changes in extracellular P_i supply. Chronic deprivation increases the synthesis of type II (22) and type III (3, 4, 23) cotransporters. In contrast, the adaptation of type II cotransporters to acute changes occurs within minutes, without de novo protein synthesis (27). It involves conformational changes of the cotransporters (25, 26) as well as sorting, endocytosis, recycling, and degradation, which are partly controlled by parathormone (28). Microtubules and microfilaments play a role in this process (18). Recently, indirect evidence has suggested that posttranslational modifications may also affect PIT-1 and PIT-2 activities (2, 32). However, this phenomenon has not been directly investigated.

In this study, we have focused on the rapid changes of PIT-2 activities in response to acute changes in phosphate supply. We observed that both phosphate uptake and A-MLV entry were affected by the phosphate concentration and by impairment of conformational changes of cell surface molecules. Variations of extracellular P_i concentrations ($[P_i]$) also modified the organization of the actin cytoskeleton, with which PIT-2 was found to be physically associated. This association determined to a significant extent the distribution of cell surface PIT-2 and appeared crucial for the internalization of the receptor in response to virus binding and for processing virus entry.

MATERIALS AND METHODS

Antibodies and reagents. Monoclonal antibodies (MAb) AC-40, P5D4 (12), Cy3-conjugated P5D4 (P5D4-Cy3), and fluorescein isothiocyanate-conjugated phalloidin (phalloidin-FITC) were from Sigma (St. Louis, Mo.). Phycoerythrin (RPE)-conjugated goat anti-mouse and anti-rat immunoglobulin G (IgG) antibodies were from Southern Biotechnology (Birmingham, Ala.). MAb 83A25 (6) was obtained from R. Evans (Rocky Mountain Laboratory, Hamilton, Mont.).

* Corresponding author. Mailing address: Laboratoire Rétrovirus et Transfert Génétique, Institut Pasteur, 28 Rue du Dr. Roux, 75724 Paris, France. Phone: 33 (0) 1 45 68 82 46. Fax: 33 (0) 1 45 68 89 40. E-mail: jmheard@pasteur.fr.

The rabbit polyclonal serum against human PIT-2 was a gift from J. V. Garcia (St. Jude Research Hospital, Memphis, Tenn.) (3). Cytochalasin D, lysophosphatidic acid (LPA), 4-chloromercuribenzoic acid (PCMB), and 4-(chloromercuri)benzene-sulfonic acid (PCMBS) were from Sigma-Aldrich (St. Louis, Mo.).

C-terminal VSV-tagged PIT-2 (PIT-2V) construction. The 11-residue epitope of the VSV-G C terminus (12) was fused to the C terminus of human PIT-2 by PCR. The C-terminal half of PIT-2, without the stop codon, was amplified with 5′-GAGCTGCGGACTCATCGG-3′ and 5′-CCCGGAATTCTCATTTTCCTAATCGATTCATTTCTATGTCTGTGTATGGGCCTGGTGGGCCCACATATGGAAGGATCCCATACATGAGAAG-3′ as positive- and negative-strand primers, respectively. The latter contained sequences encoding a spacer peptide (G-P-P-G-P), the VSV-G epitope, and a stop codon, followed by an *Eco*RI restriction site. Amplification products were digested with *Xho*I and *Eco*RI and inserted in plasmid pCDNA3 into which the PIT-2 cDNA of pOJ74 (33) had been previously transferred.

Cell lines. TE671 and TelcEB6 cells were cultured in Dulbecco modified Eagle medium (DMEM), and CHO and CEAR 13 cells (10) were cultured in Ham F-12 medium supplemented with 10% fetal bovine serum. Media with defined [P_i] were based on phosphate-free RPMI 1640 (ICN, Costa Mesa, Calif.) supplemented with 10% dialyzed fetal bovine serum and various molarities of Na_2HPO_4 and NaH_2PO_4. CHO cell clones expressing PIT-2V (CHO-PIT-2V), selected with G418 (1 mg/ml), were screened for cell surface PIT-2V expression and susceptibility to amphotropic virus infection.

Retroviruses. Amphotropic and VSV-G pseudotype stocks of a retrovirus vector containing the *nls-lacZ* gene expressed under the control of the long terminal repeat were prepared from a stable Ψ-CRIP cell clone and from TelcEB6 cells (5) transiently transfected with plasmid DNA encoding VSV-G (35), respectively. Twenty-four-hour supernatants of confluent cultures were collected, filtered through 0.45-μm-pore-size filters, and stored at −80°C until use. Infectious titers, as determined on NIH 3T3 cells, were 10^7 and 10^5 β-galactosidase focus-forming units (FFUs) per ml for the A-MLV and VSV-G pseudotypes, respectively. Amphotropic vector stocks contained soluble amphotropic envelope surface components (SUs) which are detectable by Western blotting, which can bind cell surface receptors, and which are detectable by MAb 83A25 in binding assays.

Immunoprecipitation and Western blotting. For immunoprecipitation, CHO-PIT-2V or TE671 cells were incubated for 2 h with defined [P_i]. Cells were washed with HBS (10 mM HEPES-buffered saline) with adjusted [P_i] and lysed in 1 ml of HBS with adjusted [P_i]–0.5% Triton X-100–protease inhibitors. Cell extracts were recovered with a cell scraper, kept on ice for 15 min, frozen-thawed, and incubated overnight at 4°C with AC-40 (1:300 dilution) or a control IgG2a MAb. Immune complexes were precipitated with protein A-agarose for 2 h at 4°C, washed with ice-cold phosphate-buffered saline (PBS), run on a sodium dodecyl sulfate–10% polyacrylamide gel, and analyzed by Western blotting.

For Western blotting, samples were electrophoresed on sodium dodecyl sulfate–10% polyacrylamide gels, transferred to nitrocellulose membranes, incubated overnight at 4°C with the primary antibody (rabbit anti–PIT-2 serum, 1:250 dilution, or AC-40, 1:1,000 dilution), washed, and revealed with a horseradish peroxidase-coupled secondary antibody and enhanced chemiluminescence (ECL kit from Amersham).

Virus infection experiments. Cells (5×10^4) maintained at physiological [P_i] were switched to medium containing various [P_i] or drug concentrations. After 30 min at 37°C, 100 FFUs of the vector preparation was added for 30 min in the presence of 8 μg of Polybrene per ml. Cells were incubated for 5 h with fresh medium containing equivalent [P_i] or drug concentrations. Cells were washed and further cultivated for 24 h in normal culture medium prior to 5-bromo-4-chloro-3-indolyl-β-D-galactopyranoside (X-Gal) staining and scoring of β-galactosidase-positive foci.

Phosphate uptake measurements. Cells (2×10^5) were seeded on 24-well plates and cultured overnight. After preincubation with or without phosphate, cytochalasin D, PCMB, or PCMBS for 30 min at 37°C followed by three washes with HBS, cells were incubated with 300 μl of $NaH_2{}^{32}PO_4$ (5 μCi/ml; specific activity, 200 mCi/mmol) in phosphate-free medium for 1 min at room temperature. Cells were immediately washed once with 40 mM NaH_2PO_4 in PBS and twice with PBS. Cell extracts were prepared in PBS with 1% Triton X-100, and radioactivity was counted with a 1450 Microbeta Trilux (Wallac). Data were expressed relative to the total protein concentration measured in cell extracts (bicinchoninic acid kit; Pierce, Rockford, Ill.). All experiments were performed in triplicate.

Immunofluorescence. For PIT-2 and actin determinations, 10^5 cells were seeded on coverslips and cultured overnight. After incubation in defined [P_i] for 2 h, cells were fixed in 3% formaldehyde in the same medium for 20 min at room temperature and quenched with 50 mM NH_4Cl in PBS for 10 min. Permeabilization was performed with 0.1% Triton X-100–3% formaldehyde in culture medium for 5 min at room temperature before quenching. Coverslips were placed on a 25-μl drop containing P5D4-Cy3 (1:500 dilution in 1% bovine serum albumin [BSA]–0.1% azide in PBS [PBA]) and/or phalloidin-FITC (0.25 μg/ml). The same procedure was used for internalization assays, except that cells were exposed to 30 μl of the amphotropic vector stock (multiplicity of infection [MOI], 3) for 2 h at 37°C prior to fixation and permeabilization. When used, drugs were added 30 min prior to fixation. Images were acquired with a Zeiss confocal fluorescence microscope and contrast enhanced with Adobe Photoshop 4.0 software.

Flow cytometry analysis. Virus binding assays were performed on confluent cells after incubation at various [P_i] or in the presence of various drugs for 30 min at 37°C. Cells were collected with 2 mM EDTA in HBS and exposed to the amphotropic vector stock in defined [P_i] for 30 min at 37°C or 16 h at 4°C (MOI, 3). After being washed with ice-cold PBS, cells were either labeled immediately or incubated at 37°C for various periods of time prior to being washed and labeled with MAb 83A25 (1:2 dilution) (6) for 1 h at 4°C. After being washed with ice-cold PBS, cells were stained with RPE-conjugated goat anti-rat IgG in PBA (1:150 dilution), washed, and fixed (1% formaldehyde in PBA) before analysis on a FACScan (Becton Dickinson).

Analysis of PIT-2V expression was performed by incubating cells for 3 h at 4°C with P5D4 (1:500 dilution in PBA) and then staining them with an RPE-conjugated secondary antibody. For PIT-2V internalization studies, cells were treated as for virus binding assays, except that labeling was done with MAb P5D4 (1:500 dilution).

RESULTS

We investigated the expression and the NaP_i cotransporter and amphotropic retrovirus receptor functions of PIT-2. Tagged versions of human PIT-2 (PIT-2V) were generated with the aim of detecting extracellular epitopes. The 11-amino-acid (YTDIEMNRLGK) epitope of VSV-G recognized by MAb P5D4 (13) was used for tagging. Modified PIT-2 coding sequences were inserted downstream of the human cytomegalovirus promoter and expressed in CHO cells. Immunofluorescence and flow cytometry analysis with P5D4 indicated that the tagging epitope was detectable at the outer side of the plasma membrane when inserted at the C terminus of PIT-2. This finding was not predicted by sequence analysis, which located the C terminus of PIT-2 intracellularly. Other constructs gave negative results. A cell clone stably expressing the C-terminally tagged version of PIT-2 (PIT-2V) was isolated. Immunoprecipitation of ^{35}S-methionine- and ^{35}S-cysteine-labeled CHO-PIT-2V cell extracts with P5D4 revealed a 70-kDa PIT-2-specific signal (data not shown). PIT-2V could not be detected by Western blotting with P5D4, but a strong signal was specifically revealed with a rabbit serum raised against the intracellular loop of human PIT-2 (3). Whereas the endogenous PIT-2 molecule is not functional for amphotropic virus binding and infection in parental CHO cells, CHO-PIT-2V clones bound amphotropic envelope glycoproteins efficiently (Fig. 1B, E, and H). Binding was threefold higher than in human TE671 cells, which express 1.4×10^5 amphotropic receptors at the surface (data not shown) (1). Exposure of CHO-PIT-2V clones to an amphotropic pseudotype of a retrovirus vector carrying *nls-lacZ* induced β-galactosidase-positive foci (Fig. 1C, F, and I). The uptake of extracellular $Na_2H^{32}PO_4$ was eightfold higher in CHO-PIT-2V clones than in parental CHO cells (Fig. 1A), indicating that PIT-2V participated significantly in transmembrane P_i transport in CHO-PIT-2V cells. Taken together, these data indicated that PIT-2V was efficiently expressed and functioned as a phosphate transporter and as a receptor for amphotropic retroviruses in CHO-PIT-2V cells.

Effects of extracellular [P_i] on PIT-2 functions. We examined whether PIT-2V functions are affected when extracellular [P_i] vary. Intracellular $Na_2H^{32}PO_4$ uptake, cell surface binding of amphotropic envelope glycoprotein, and cell susceptibility to retrovirus infection were examined less than 6 h after the cells were switched from the physiological extracellular Na_2HPO_4 concentration (1 mM) to medium containing Na_2HPO_4 concentrations ranging from 0 to 40 mM. $Na_2H^{32}PO_4$ uptake was increased twofold 30 min after the cells were switched to 0 mM Na_2HPO_4 (Fig. 1D). The level of infection with an amphotropic vector increased to 125% ± 5% (*n*, 3) the initial value after 5 h (Fig. 1F). Both $Na_2H^{32}PO_4$ uptake and the level of infection were rapidly reduced after the cells were switched

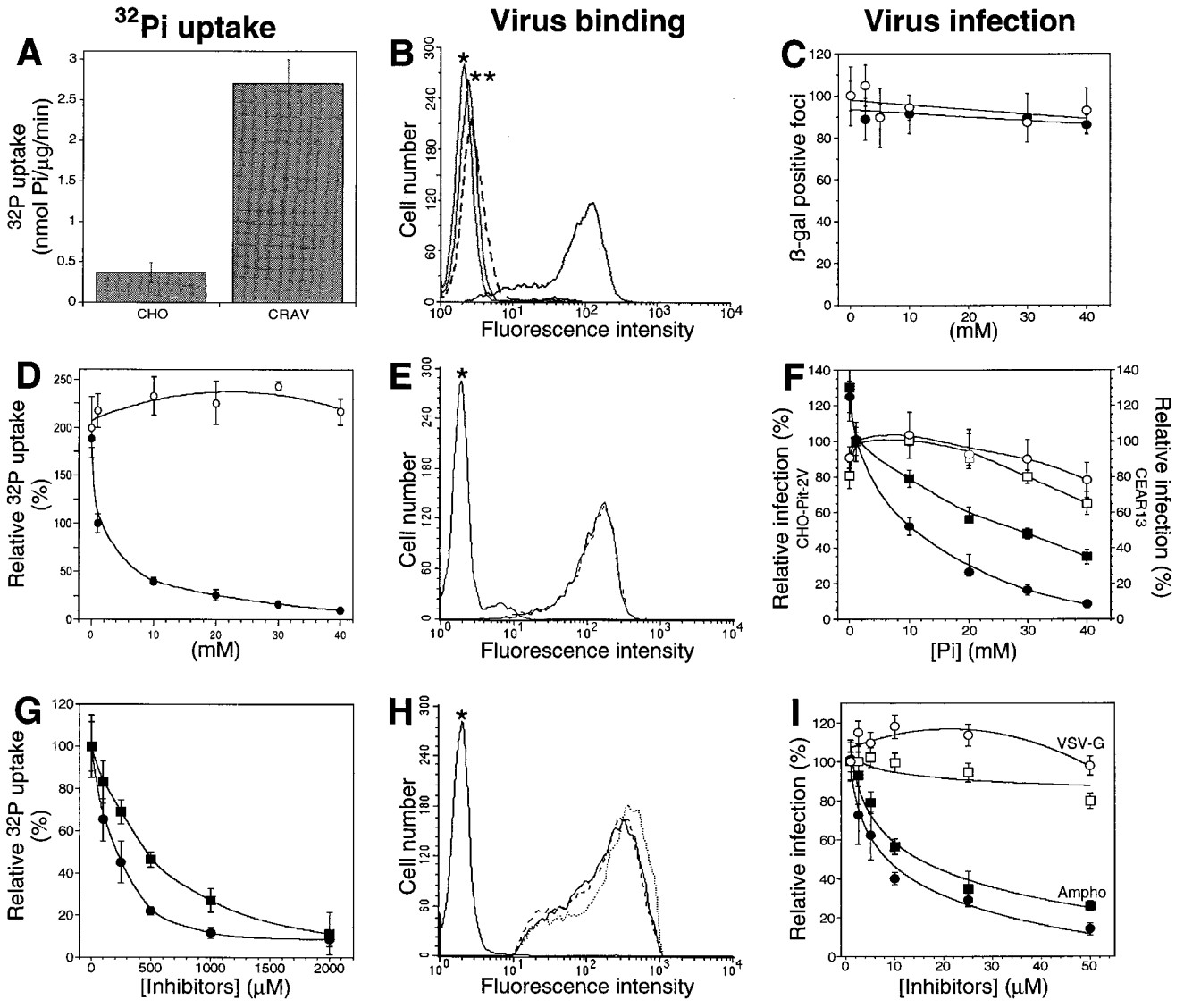

FIG. 1. Extracellular [P_i] and inhibitors of P_i transport affect PIT-2V functions. (A to C) Control experiments performed with 1 mM [P_i] in the absence of drug. (A) Increased P_i uptake in CHO-PIT-2V cells (CRAV) compared to parental CHO cells (CHO). (B) Flow cytometry revealed amphotropic envelopes bound to CHO-PIT-2V cells (solid line and no asterisks) but not to parental CHO cells (broken line). Asterisks indicate signals without viral envelopes. (C) Exposure to an amphotropic *lacZ* retrovirus vector induced β-galactosidase-positive foci on CHO-PIT-2V cells but not parental CHO cells (data not shown). Equal numbers were scored with various concentrations (*x* axis) of NaCl (closed circles) or $NaHCO_2$ (open circles). (D to F) CHO-PIT-2V cells maintained at physiological [P_i] (1 mM) were switched to medium containing the indicated [P_i] (*x* axis) for 30 min at 37°C. (D) $NaH_2{}^{32}PO_4$ uptake was affected by changing the Na_2HPO_4 concentration (closed circles; sulfate, 0.4 mM) but not the Na_2SO_4 concentration (open circles; phosphate, 0 mM). (E) Equivalent binding of amphotropic envelopes at 0 mM (solid line) and 40 mM (broken line) [P_i]. (F) Infection efficiency for CHO-PIT-2V cells (closed circles; 100%, 97 ± 9 FFUs) or CEAR 13 cells (closed squares; 100%, 265 ± 21 FFUs) with an amphotropic vector and different [P_i]. In contrast, infection of CHO-PIT-2V cells with a VSV-G pseudotype (open circles; 100%, 90 ± 7 FFUs) or of CEAR 13 cells with an ecotropic pseudotype (open squares; 100%, 179 ± 5 FFUs) was unaffected. (G to I) To CHO-PIT-2V cells maintained at physiological [P_i] (1 mM) were added the indicated concentrations of PCMB (squares) or PCMBS (circles) for 30 min at 37°C. (G) Drugs inhibited Na_2HPO_4 uptake. (H) Unmodified binding of amphotropic envelopes (solid line, no drug; broken line, 200 μM PCMB; dotted line, 200 μM PCMBS). (I) Drugs inhibited infection with an amphotropic (Ampho) vector (closed symbols; 100%, 125 ± 12 FFUs) but not with a VSV-G pseudotype (open symbols; 100%, 95 ± 17 FFUs). Data are means ± standard deviations for triplicate experiments.

to high [P_i] (Fig. 1D and F). Reduction was not observed in control experiments performed with equivalent concentrations of Na_2SO_4, NaCl, or $NaHCO_2$, indicating that this effect was not a consequence of increased osmolality but rather was specific for phosphate (Fig. 1C and D). Virus particles interacting with PIT-2V were specifically affected, as shown by the absence of an effect of [P_i] on control pseudotypes of MLV particles bearing VSV-G or ecotropic viral envelopes incubated on CHO cells expressing the mCAT1 cell surface receptor (CEAR 13) (10) (Fig. 1F). Amounts of cell-bound viral envelopes were not affected at high [P_i] (Fig. 1E), indicating that the reduction of phosphate transport and virus entry was due not to a decreased number but rather to a decreased activity of cell surface PIT-2V molecules.

As the substrates for the transport reaction, Na and P_i induce conformational changes of type II NaP_i cotransporters, which could be identified by tryptophan fluorescence quenching (24). Depending on the residues with which they react, sulfhydryl reagents, such as PCMB and PCMBS, affect these conformational changes and operate as noncompetitive inhib-

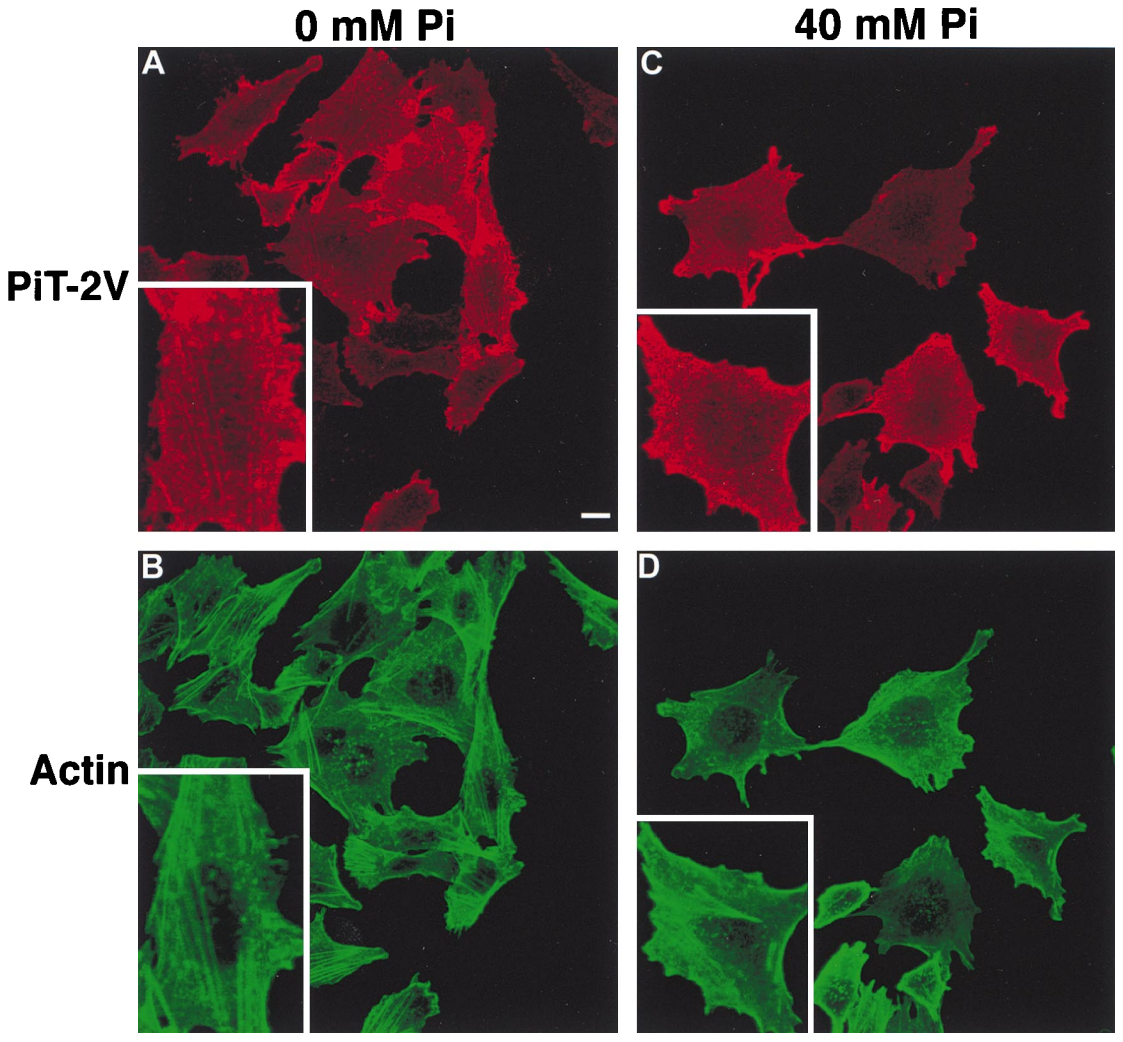

FIG. 2. Effects of extracellular [P_i] on the cell surface distribution of PIT-2V. CHO-PIT-2V cells maintained at physiological [P_i] (1 mM) were switched to medium containing the indicated [P_i] for 2 h at 37°C and analyzed by confocal fluorescence microscopy for cell surface PIT-2V expression with MAb P5D4-Cy3 (A and C) and for intracellular actin filament structure with phalloidin-FITC (B and D). The same fields are shown in panels A and B and in panels C and D. Inserts contain enlargements of the same areas. Bar, 5 μm.

itors of the cotransport reaction (16, 26). We examined whether these drugs also affect PIT-2V functions. $Na_2H^{32}PO_4$ uptake and susceptibility to amphotropic virus infection were measured with CHO-PIT-2V cells exposed for 30 min to various concentrations of these drugs. Fifty percent inhibition of P_i uptake was observed with 500 μM PCMB or 250 μM PCMBS (Fig. 1G). Inhibition of amphotropic virus infection was obtained at much lower concentrations (50% inhibitory concentration, 10 μM) (Fig. 1I). Endogenous P_i transport systems may account for this difference. In contrast, envelope glycoprotein binding was unaltered at 200 μM PCMB or PCMBS (Fig. 1H), and cell infection with control VSV-G pseudotypes was not affected (Fig. 1I). Thus, impairing substrate-induced conformational changes of cell surface PIT-2V affected both phosphate transport and virus entry but neither the number of molecules present at the cell surface nor the binding of amphotropic envelope glycoproteins. These results suggest that conformational changes of cell surface PIT-2 affect its activity.

Effect of [P_i] on the association of PIT-2 with the actin network. We examined whether changes in extracellular [P_i] modify the PIT-2V cell surface expression pattern. CHO-PIT-2V cells maintained at physiological [P_i] were switched to 0 or 40 mM Na_2HPO_4 for 60 min and stained for cell surface PIT-2V with P5D4 without permeabilization of the plasma membrane. Cells were observed by immunofluorescence (Fig. 2A and C). At 0 mM Na_2HPO_4, confocal microscopy revealed linear arrays of PIT-2V signals at the cell surface. Such images were not observed at 40 mM. An intermediate phenotype was seen for cells maintained at 1 mM (data not shown). Therefore, the cell surface distribution of PIT-2V was affected by extracellular [P_i].

Since the PIT-2V pattern at 0 mM Na_2HPO_4 was reminiscent of that of membrane proteins associated with intracellular actin filaments, CHO-PIT-2V cells were doubly stained with P5D4 and fluorescein-conjugated phalloidin, which enters nonpermeabilized cells. Phosphate deprivation had a striking effect on the actin network (Fig. 3A to C). At 0 mM Na_2HPO_4, actin was distributed as bright linear arrays in stress fibers (Fig. 2B and 3A). At 40 mM Na_2HPO_4, actin staining was diffuse, with few visible structures (Fig. 2D and 3C). Similar observations were made for parental CHO cells, indicating that this phenomenon was independent of the presence of PIT-2V (data

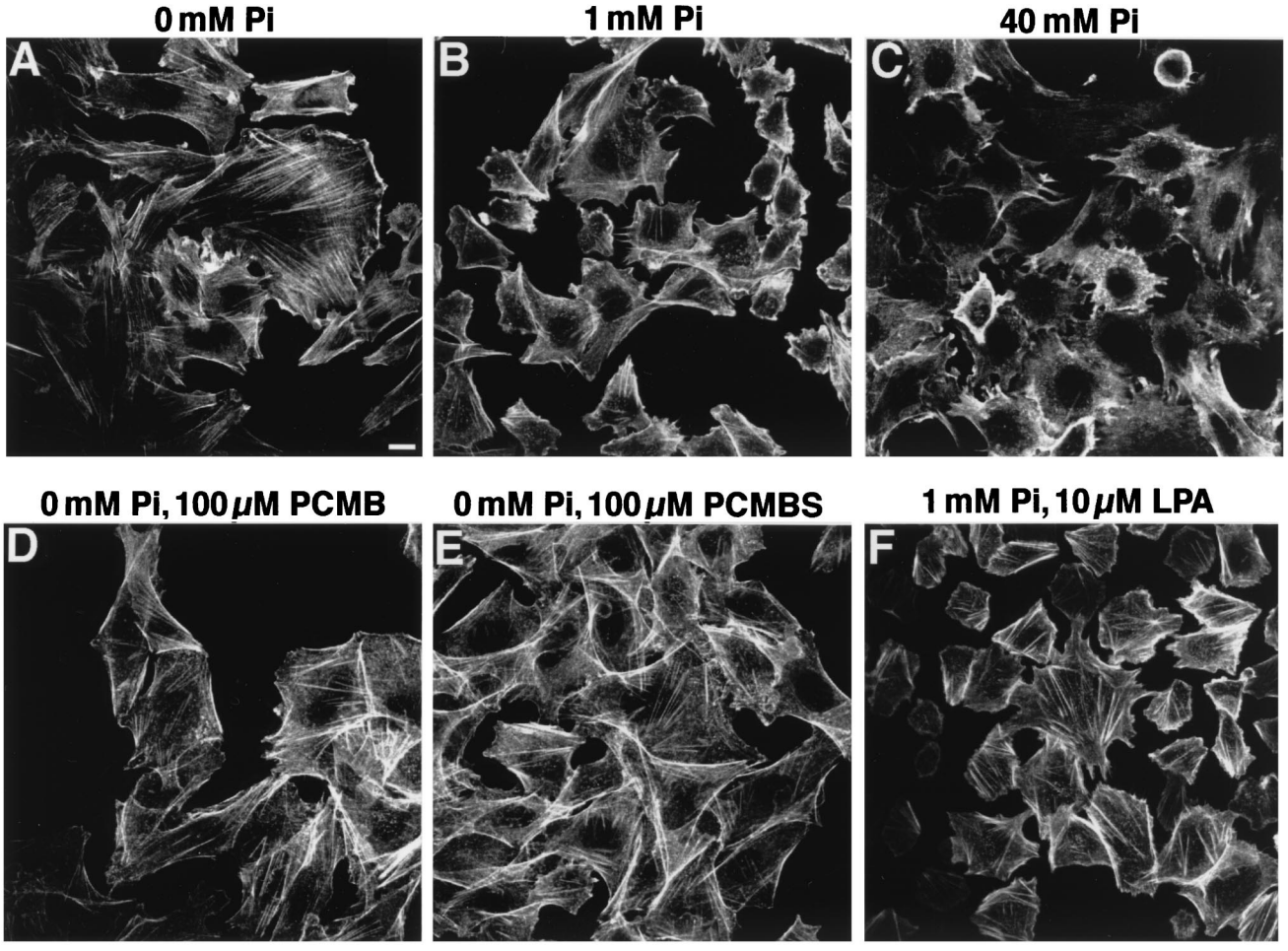

FIG. 3. Effects of extracellular [P_i], PCMB, PCMBS, and LPA on the actin network. CHO-PIT-2V cells maintained at physiological [P_i] (1 mM) were switched to the indicated conditions for 30 min, stained with phalloidin-FITC, and examined by fluorescence microscopy. Bar, 5 μm.

not shown). Cell treatment with PCMB and PCMBS for 30 min did not affect the actin network (Fig. 3D and E).

In CHO-PIT-2V cells, PIT-2V staining was precisely localized with that of actin stress fibers at 0 mM Na_2HPO_4 (Fig. 2A and B). Although some actin structures were visible in cells incubated with 40 mM Na_2HPO_4, PIT-2V staining was not localized with these structures (Fig. 2C and D). These data indicated that phosphate deprivation stimulated the formation of actin stress fibers and resulted in the apparent colocalization of PIT-2V and actin filaments.

The colocalization of PIT-2V with actin suggested that the molecules can be physically associated. This possibility was investigated by coimmunoprecipitation experiments. CHO-PIT-2V cells were incubated for 2 h with 0, 1, or 40 mM Na_2HPO_4, and cell extracts were prepared at the same [P_i]. PIT-2V was revealed by Western blotting with rabbit anti–PIT-2 antiserum. The amounts of PIT-2V were independent of [P_i] (Fig. 4A), confirming the observation made by immunofluorescence. Actin was revealed in the same extracts with MAb AC-40. The actin signal was slightly more intense at 0 mM than at 1 or 40 mM Na_2HPO_4. Cell extracts were precipitated with the antiactin MAb AC-40, and immune complexes were analyzed for the presence of PIT-2V by Western blotting. A 70-kDa signal comigrating with PIT-2V was detected in CHO-PIT-2V cells (Fig. 4B) but not in control CHO cells (data not shown), indicating the existence of PIT-2V–actin molecular complexes. This signal was more intense in extracts prepared from cells incubated at 0 mM rather than at 1 or 40 mM Na_2HPO_4. Similar experiments were performed with TE671 cells. The detection of an endogenous human PIT-2 signal required a much longer exposure than that of PIT-2V in CHO cells (Fig. 4A). A 70-kDa signal comigrating with PIT-2 was detected by coimmunoprecipitation at 0 mM but not at 1 or 40 mM (Fig. 4B), confirming the existence of PIT-2–actin complexes, which were more easily detected under phosphate-deprived conditions.

The association of PIT-2 with actin filaments was confirmed by treating cells with cytochalasin D, a drug which penetrates nonpermeabilized living cells and disorganizes the actin network. CHO-PIT-2V cells were incubated for 2 h with 0 or 40 mM Na_2HPO_4, and cytochalasin D (1 μg/ml) was added during the last 45 min. Cells were doubly stained with P5D4 and fluorescein-conjugated phalloidin and then analyzed by confocal microscopy. Cytochalasin D had a dramatic effect on the cell surface PIT-2V distribution (Fig. 4C). At 0 mM Na_2HPO_4, PIT-2V staining was condensed in large aggregates and at the cell margins. Similar aspects were observed at 40 mM Na_2HPO_4, except that the aggregates were smaller and the staining at the cell margins was more intense. These results showed that the cell surface distribution of PIT-2V depended on the organization of the intracellular actin network. Since

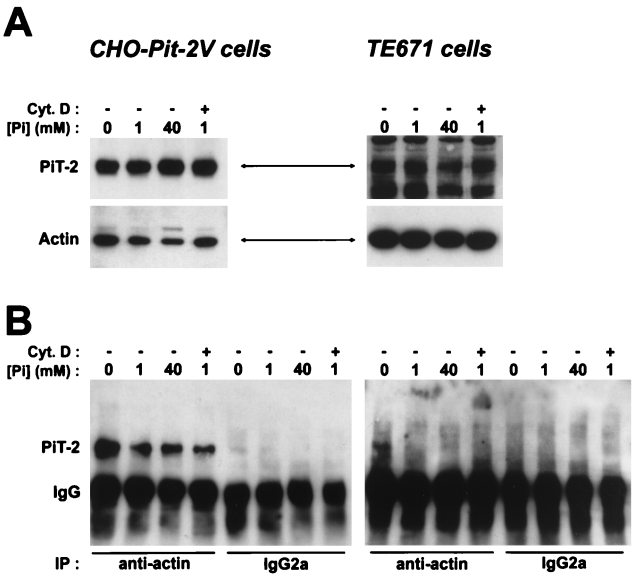

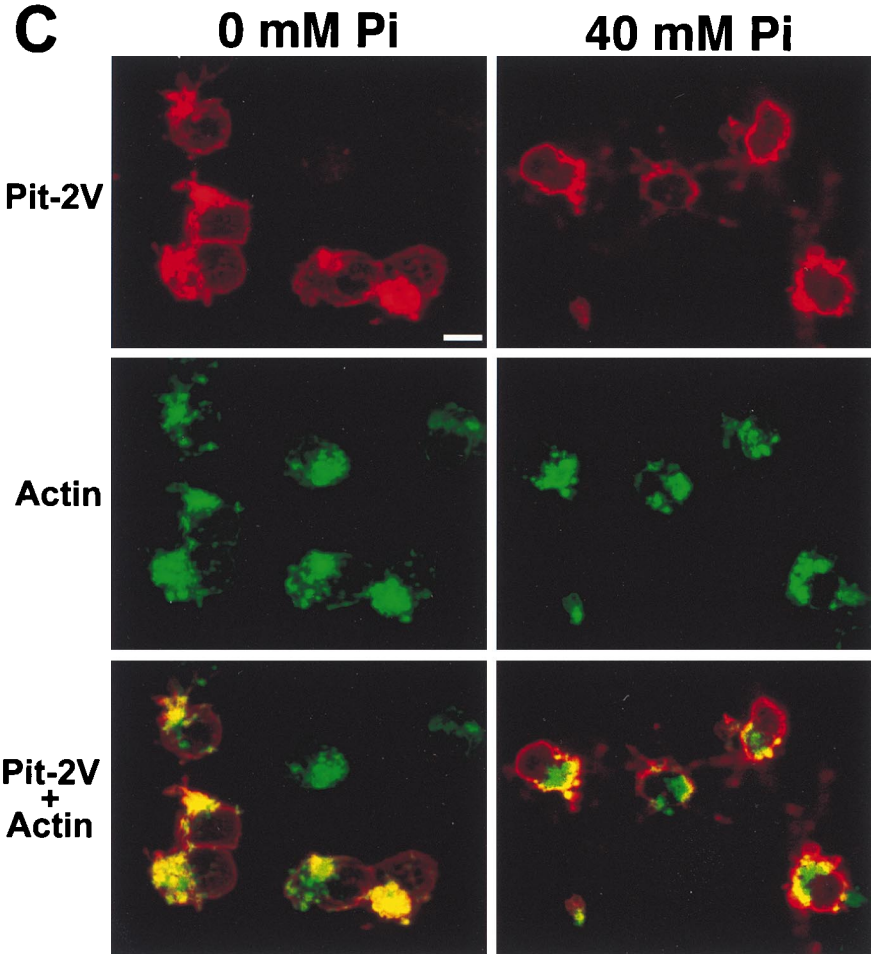

FIG. 4. Association of PIT-2 with actin. (A and B) CHO-PIT-2V and TE671 cells were incubated at the indicated [P_i] for 2 h. Cytochalasin D (Cyt. D) (1 μg/ml) was added (+) or not added (−) 45 min prior to analysis. (A) Western blot with rabbit anti–PIT-2 serum (top panel; exposures: CHO-PIT-2V, 15 s, and TE671, 15 min) and MAb AC-40 (bottom panel; exposure: 15 s). (B) Immunoprecipitation (IP) with AC-40 or a nonrelevant MAb (IgG2a) followed by Western blotting with rabbit anti–PIT-2 serum. Signals corresponding to PIT-2 and IgG are indicated. Exposures: CHO-PIT-2V, 3 min, and TE671, 10 min. (C) Confocal immunofluorescence microscopy of CHO-PIT-2V cells treated with cytochalasin D. Top panels show P5D4-Cy3 staining (red); middle panels show phalloidin-FITC staining (green); and bottom panels show superimposed staining (yellow). Bar, 5 μm.

actin and PIT-2V staining colocalized in aggregates but not at the cell margins, it is likely that only a fraction of cell surface PIT-2V molecules was associated with actin. More apparent colocalization at 0 mM than at 40 mM Na_2HPO_4 suggested that the proportion of PIT-2V molecules associated with actin increased at low [P_i]. At 1 mM Na_2HPO_4, coimmunoprecipitation experiments detected roughly equivalent amounts of PIT-2V associated with actin in the presence and in the ab-

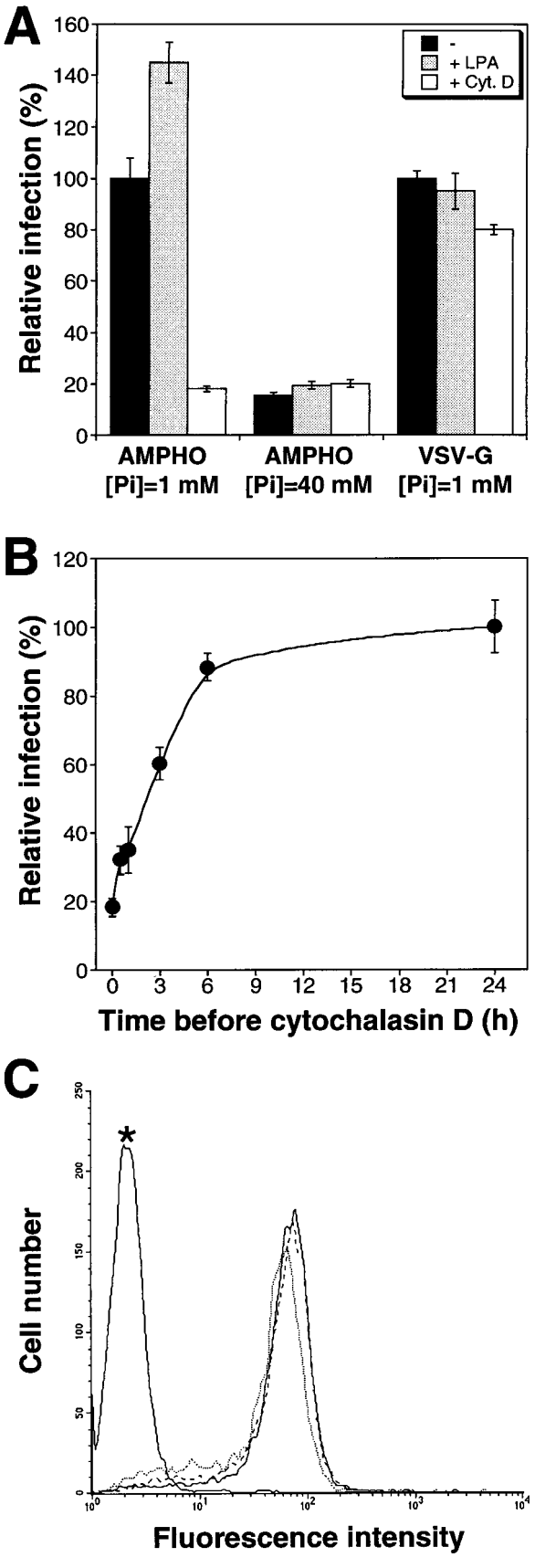

sence of cytochalasin D (Fig. 4B), indicating that cytochalasin D affected the cell surface distribution of PIT-2V but not the proportion of molecules associated with actin.

Effects of actin organization on PIT-2V functions. We examined whether drugs modifying the organization of the actin network affect PIT-2V functions. CHO-PIT-2V cells were incubated with cytochalasin D (1 μg/ml), an actin-desorganizing agent, or with LPA, a drug stimulating actin stress fiber formation (11). Induction of actin polymerization by 10 μM LPA was verified for CHO-PIT-2V cells (Fig. 3E). Equivalent amounts of amphotropic retrovirus envelope bound to untreated cells and to cells treated with cytochalasin D or LPA, indicating that these drugs did not modify the number of receptors present at the cell surface (Fig. 5C). $Na_2H^{32}PO_4$ uptake was not significantly modified by cytochalasin D or LPA (data not shown). Susceptibility to amphotropic virus infection at 1 and 40 mM Na_2HPO_4 was studied (Fig. 5A). At 1 mM Na_2HPO_4, the level of infection was strongly decreased in the presence of cytochalasin D and increased 1.5-fold in the presence of LPA. At 40 mM Na_2HPO_4, actin-modifying drugs were not active for virus infection. Control pseudotypes bearing VSV-G were not affected by cytochalasin D or LPA. Since the effects of cytochalasin D are reversible, we determined the window of time during which infection with amphotropic virus was impaired. Data indicated that cytochalasin D was effective between 0 and 3 h after exposure to the virus (Fig. 5B). These data indicated that the actin cytoskeleton plays a role in virus entry through PIT-2 but not in the transmembrane transport of P_i.

Internalization of PIT-2 in response to virus particle binding. We explored further the roles of extracellular [P_i], PIT-2 conformational changes, and actin microfilaments in amphotropic virus entry. Cell surface PIT-2V expression in CHO-PIT-2V cells after exposure to amphotropic virus was examined. Amphotropic virus particles were allowed to bind receptors at 4°C. Virus binding was controlled by staining with the anti-SU MAb 83A25 (data not shown). After the elimination of unbound particles by washing, cells were warmed to 37°C for various periods of time and at various [P_i] in order to trigger virus entry. Cell surface PIT-2V levels were analyzed with P5D4 over time by flow cytometry (Fig. 6). In control experiments without virus exposure, cell surface PIT-2V levels were stable over a 6-h incubation period at 37°C. Analysis immediately after virus exposure (time zero) indicated that PIT-2V was accessible to P5D4 when virus particles were attached to the cell surface. Cells incubated with 0 mM Na_2HPO_4 showed a decrease (65% reduction) of the cell surface PIT-2V signal at 1 h; the signal became almost undetectable after 4 h. At 1 mM Na_2HPO_4, cell surface PIT-2V levels decreased more slowly but were also undetectable after 6 h. In contrast, the

FIG. 5. Effects of extracellular [P_i] and of drugs modifying the actin network on A-MLV binding and infection. CHO-PIT-2V cells were incubated at the indicated [P_i] for 30 min without (−) or with cytochalasin D (Cyt. D) (1 μg/ml) or LPA (10 μM) prior to exposure to A-MLV (AMPHO) or VSV-G pseudotypes for 30 min at 37°C under the same conditions. (A) Infection efficiency. The virus input was 100 FFUs (MOI, 0.01). Cells were incubated for 5 h under the same conditions, washed, and grown in normal medium. β-Galactosidase-positive foci at 1 mM P_i were scored 24 h later. Reference values (100%) were 105 ± 8 foci for A-MLV and 95 ± 5 foci for VSV-G. Data are the mean percentages of maximal infection ± standard deviations (n = 3). (B) Kinetics of virus entry. The conditions were the same as those in panel A, except that cytochalasin D (1 μg/ml) was added immediately after A-MLV exposure (time zero) or after the indicated periods of time. The score at 24 h (100% value) was 91 ± 7 foci. (C) Virus envelope binding assay. Cell-bound A-MLV envelopes were analyzed by flow cytometry with MAb 83A25 30 min after the addition of the virus input (30 μl; MOI, 3). Solid line, no drug added; dotted line, cytochalasin D (1 μg/ml);broken line, LPA (10 μM). The asterisk indicates staining without viral envelopes.

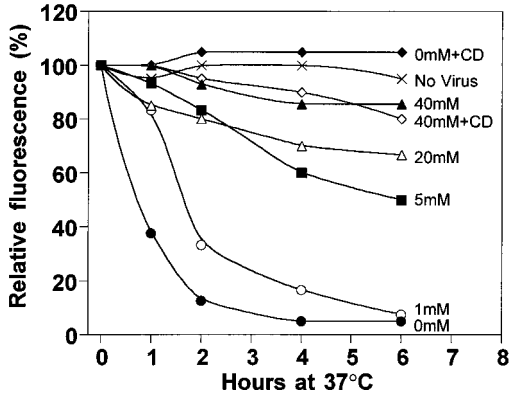

FIG. 6. Analysis of cell surface PIT-2V after exposure to A-MLV. CHO-PIT-2V cells were incubated at the indicated [P_i] for 2 h in the absence or in the presence of cytochalasin D (CD) (1 μg/ml), detached, and exposed to medium containing A-MLV particles (MOI, 3) and soluble envelopes at 4°C for 16 h, and then extensively washed. Cells were stained with P5D4-Cy3 and analyzed by flow cytometry immediately, providing the 100% reference fluorescence level, or after incubation under defined [P_i] and cytochalasin D conditions for the indicated periods of time at 37°C (hours at 37°C). Data are from one representative experiment of at least three.

cell surface PIT-2V signal was stable over time at 40 mM Na_2HPO_4. Intermediate behaviors were observed at intermediate [P_i] (5 and 20 mM). After previous treatment with cytochalasin D (1 μg/ml), cell surface PIT-2V expression was stable over time in medium containing 1 mM Na_2HPO_4.

We examined whether the disappearance of cell surface PIT-2V was due to receptor internalization. CHO-PIT-2V cells incubated with 0 or 40 mM Na_2HPO_4 were exposed to amphotropic virus particles for 2 h at 37°C, washed, and permeabilized before PIT-2V staining with P5D4 and immunofluorescence microscopy. In cells exposed to virus at 40 mM Na_2HPO_4, PIT-2V staining was diffuse, with a slightly more intense signal at the cell margins. This aspect was very similar to that observed for control cells not exposed to virus (Fig. 7C and D). In contrast, cell surface staining disappeared in cells exposed to virus at 0 mM Na_2HPO_4; the signal was concentrated in perinuclear spots (Fig. 7A and B). This aspect was highly suggestive of the internalization of PIT-2V in intracellular vesicles.

PIT-2V internalization in response to virus exposure was investigated in the presence of drugs affecting phosphate transport or actin organization. Cells were incubated with 0 mM Na_2HPO_4 for 1 h, with or without drugs during the second 30 min, and then exposed to virus particles in the same medium for 2 h at 37°C before fixation, permeabilization, and staining of PIT-2V with P5D4. Receptor internalization was abolished in the presence of the phosphate transport inhibitors PCMB and PCMBS (100 μM) (Fig. 7E to H). This result suggested that drugs affecting PIT-2V conformational changes also affect receptor internalization in response to virus particle binding. Similar observations were made for cells treated with cytochalasin D (1 μg/ml) (Fig. 7I and J), indicating that the integrity of the actin network was required for receptor internalization in response to virus binding as well as for cell infection.

DISCUSSION

We have obtained evidence for posttranslational regulation of the activity of PIT-2, a type III NaP_i cotransporter also involved in the entry of amphotropic retroviruses into target cells. Posttranslational modifications modulating the transmembrane transport of P_i have been described previously for type II NaP_i cotransporters (14, 17, 21). Our experiments were performed with a tagged version of human PIT-2 expressed in CHO cells. Both activities of PIT-2, namely, the transmembrane transport of P_i and the entry of amphotropic retroviruses, were rapidly modulated following changes in extracellular [P_i]. Modulation involved changes in neither the total amounts of PIT-2 nor the number of cell surface molecules, as shown by Western blotting with cell extracts and by flow cytometry analysis of amphotropic envelope glycoprotein binding. Therefore, we assumed that the modulation of PIT-2 activities resulted from modifications of the conformation and/or the organization of cell surface molecules. This hypothesis was supported by the inhibition of both activities in the presence of drugs impairing conformational changes of NaP_i cotransporters and by the observed modification of the cell surface distribution pattern of a tagged version of PIT-2 in response to changes in extracellular [P_i].

The redistribution of cell surface PIT-2 in response to P_i deprivation was associated with a reorganization of the actin network. In parental CHO cells as well as in CHO-PIT-2V and TE671 cells, the abundance of actin stress fibers was inversely related to extracellular [P_i]. A similar observation has been reported previously (29). PIT-2V staining was precisely localized with that of actin stress fibers, while coimmunoprecipitation experiments demonstrated a physical association of PIT-2 with actin. These results support the assumption that the cell surface distribution of PIT-2 is determined to some extent by the organization of the actin network. Consistently, the cell surface distribution of PIT-2 was severely affected by the actin-disorganizing drug cytochalasin D, while its association with actin was maintained. Extracellular [P_i] not only affected the organization of the actin network but also modulated the proportion of PIT-2 molecules associated with actin microfilaments. Thus, in the presence of phosphate deprivation, PIT-2 molecules were more frequently associated with highly polymerized actin microfilaments. Whether PIT-2 binds actin directly or through connections established by actin binding proteins is currently being investigated.

Indications that the cytoskeleton plays a role at early stages of the viral life cycle have been previously obtained for other retroviruses, including ecotropic MLV (9), lentiviruses (7), and spumaviruses (31). However, the mechanisms remain mostly undocumented. We showed that the receptor for A-MLV is physically associated with actin and that the entry of virus particles is more efficiently processed by PIT-2 when the actin network is highly polymerized. Cell infection was inhibited by high extracellular [P_i] and cytochalasin D, whereas it was stimulated by low extracellular [P_i] and LPA. These effects were specific for PIT-2, since infection efficiency was affected neither by the extracellular concentration of other anions nor when virus entry was mediated by another receptor. Alteration of cell infection was not the consequence of altered binding of

FIG. 7. Internalization of PIT-2 in response to A-MLV exposure. CHO-PIT-2V cells were incubated at the indicated [P_i] for 4 h at 37°C and not exposed (left panels) or exposed (right panels) to medium containing A-MLV particles (MOI, 3) and soluble envelopes for the last 2 h. When indicated, drugs were added for 30 min prior to virus exposure. Cyt. D, cytochalasin D. After fixation and permeabilization, cells were stained with P5D4-Cy3 and analyzed by confocal fluorescence microscopy. Data are from one representative experiment of three. Bar, 5 μm.

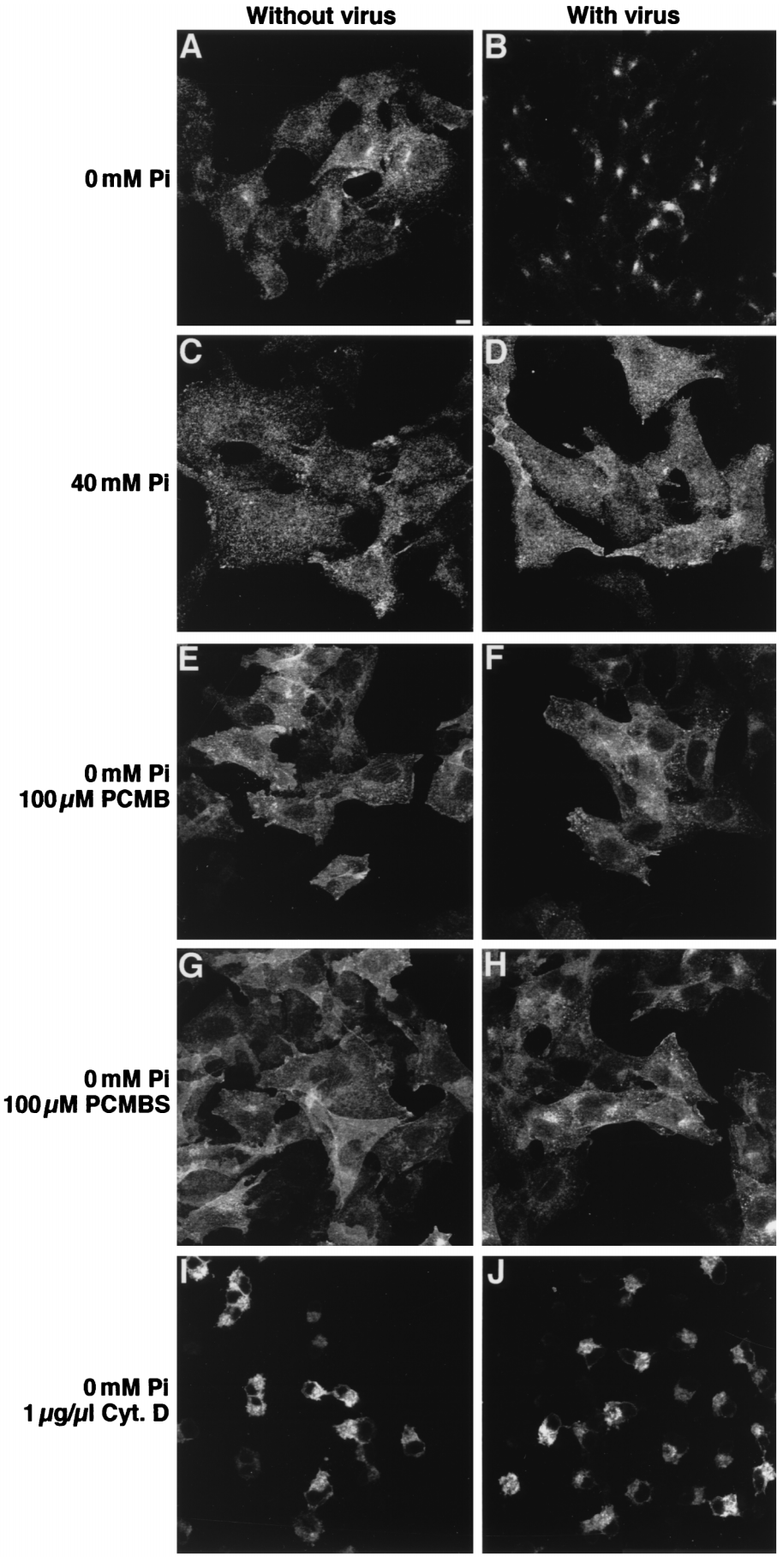
Without virus
With virus
A
B
0 mM Pi
C
D
40 mM Pi
E
F
0 mM Pi
100 μM PCMB
G
H
0 mM Pi
100 μM PCMBS
I
J
0 mM Pi
1 μg/μl Cyt. D

virus particles but rather was due to the altered efficiency of the entry process. Impaired virus entry was consistently associated with impaired internalization of PIT-2 in response to virus particle binding, suggesting that these phenomena may be related. However, the involvement of PIT-2 internalization in virus entry raises questions. Indeed, in contrast to ecotropic or VSV-G pseudotypes, amphotropic particles do not require internalization into acidic vesicles for fusion, leading to the assumption that fusion takes place at the cell surface (19, 30). According to this view, receptor internalization should be secondary to fusion, playing roles in infection other than mediating virus entry, for example, activating signal transduction pathways or degrading receptor-bound virus particles in lysosomes. Alternatively, pH-independent fusion could take place in vesicles, where multiple envelope-receptor interactions may be facilitated by physical constraints. Receptor internalization would then directly participate in the entry process.

The analysis of cell surface PIT-2V by flow cytometry indicated that raising extracellular [P_i] did not down-regulate the expression of the cotransporter, at least during the first 6 h. Although constant recycling cannot be ruled out, this result suggests that the rapid adaptive changes of the NaP_i cotransport activity of PIT-2 are achieved without modification of the number of cell surface molecules. Therefore, PIT-2 molecules present at the cell surface can be either activated or inactivated. Molecular organizations which support the activated and inactivated states of PIT-2 are unknown. However, treatment with PCMB or PCMBS, which impairs the conformational changes of type II NaP_i cotransporters induced by P_i, inhibit P_i transport and virus entry mediated by PIT-2. It is therefore likely that conformational changes participate in activation. One plausible hypothesis is that inactive molecules are monomers which may interact with each other or with other partners to form active complexes, as was previously proposed for type II NaP_i cotransporters (8, 34). PCMB and PCMBS could interfere with the formation of such complexes. Interestingly, these drugs affected P_i transport, receptor internalization in response to virus particle binding, and virus entry, suggesting that similar molecular constraints influence the occurrence of these various events. In contrast, virus particle binding was not affected by PCMB and PCMBS, indicating that binding and entry have different requirements. This result is consistent with our previous observations showing a dissociation of the binding and entry processes (1).

In conclusion, this study shows that the transmembrane transport of P_i and the entry of amphotropic retroviruses mediated by PIT-2 require the presence of active forms of the molecule at the cell surface. Moreover, efficient processing of retrovirus entry involves the association of the receptor with a highly polymerized actin network.

ACKNOWLEDGMENTS

We are grateful to E. Perec for assistance with confocal microscopy, to J. V. Garcia for providing the rabbit anti–PIT-2 serum, to D. Kabat for the gift of the CEAR 13 cell line, and to O. Schwartz for critical reading of the manuscript.

This work was supported by grants from the Agence National de Recherche contre le SIDA (ANRS) and Sidaction. P.R. is a fellow of Fundação para a Ciência e Tecnologia (Portugal).

REFERENCES

1. **Battini, J. L., P. Rodrigues, R. Müller, O. Danos, and J. M. Heard.** 1996. Receptor-binding properties of a purified fragment of the 4070A amphotropic murine leukemia virus envelope glycoprotein. J. Virol. **70:**4387–4393.
2. **Boyer, C. J. C., A. Baines, E. Beaulieu, and R. Béliveau.** 1998. Immunodetection of a type III sodium-dependent phosphate cotransporter in tissues and OK cells. Biochim. Biophys. Acta **1368:**73–83.
3. **Chien, M. L., J. L. Foster, J. L. Douglas, and J. V. Garcia.** 1997. The amphotropic murine leukemia virus receptor gene encodes a 71-kilodalton protein that is induced by phosphate depletion. J. Virol. **71:**4564–4570.
4. **Chien, M. L., E. O'Neill, and J. V. Garcia.** 1998. Phosphate depletion enhances the stability of the amphotropic murine leukemia virus receptor mRNA. Virology **240:**109–117.
5. **Cosset, F. L., Y. Takeuchi, J. L. Battini, R. A. Weiss, and M. K. Collins.** 1995. High-titer packaging cells producing recombinant retroviruses resistant to human serum. J. Virol. **69:**7430–7436.
6. **Evans, L. H., R. P. Morrison, F. G. Malik, J. Portis, and W. Britt.** 1990. A neutralizable epitope common to the envelope glycoproteins of ecotropic, polytropic, xenotropic, and amphotropic murine leukemia viruses. J. Virol. **64:**6176–6183.
7. **Iyengar, S., J. E. K. Hildreth, and D. Schwartz.** 1998. Actin-dependent receptor colocalization required for human immunodeficiency virus entry into host cells. J. Virol. **72:**5251–5255.
8. **Jette, M., V. Vachon, M. Potier, and R. Béliveau.** 1996. The renal sodium/phosphate symporters: evidence for different functional oligomeric states. Biochemistry **35:**15209–15214.
9. **Kizhatil, K., and L. M. Albritton.** 1997. Requirements for different components of the host cell cytoskeleton distinguish ecotropic murine leukemia virus entry via endocytosis from entry via surface fusion. J. Virol. **71:**7145–7156.
10. **Kozak, S. L., D. C. Siess, P. Kavanaugh, A. D. Miller, and D. Kabat.** 1995. The envelope glycoprotein of an amphotropic murine retrovirus binds specifically to the cellular receptor/phosphate transporter of susceptible species. J. Virol. **69:**3433–3440.
11. **Kranenburg, O., M. Poland, M. Gebbink, L. Oomen, and W. H. Moolenaar.** 1997. Dissociation of LPA-induced cytoskeletal contraction from stress fiber formation by differential localization of RhoA. J. Cell Sci. **110:**2417–2427.
12. **Kreis, T. E.** 1986. Microinjected antibodies against the cytoplasmic domain of vesicular stomatitis virus glycoprotein block its transport to the cell surface. EMBO J. **5:**931–941.
13. **Kreis, T. E., and H. F. Lodish.** 1986. Oligomerization is essential for transport of vesicular stomatitis virus glycoprotein to the cell surface. Cell **46:**1929–1937.
14. **Levi, M., M. Lotscher, V. Sorribas, M. Custer, M. Arar, B. Kaissling, H. Murer, and J. Bider.** 1994. Cellular mechanisms of acute and chronic adaptation of rat renal Pi transporter to alterations in dietary Pi. Am. J. Physiol. **267:**900–908.
15. **Li, H., and Z. Xie.** 1995. Molecular cloning of two rat Na+/Pi cotransporters: evidence for differential tissue expression of transcripts. Cell. Mol. Biol. Res. **41:**451–460.
16. **Loghman-Adham, M.** 1991. Characterization of essential sulfhydryl groups of rat Na-Pi cotransporter. Am. J. Physiol. **260:**874–882.
17. **Loghman-Adham, M., G. T. Motock, P. Wilson, and M. Levi.** 1995. Characterization of Na(+)-phosphate contransporters in renal cortical endosomes. Am. J. Physiol. **269:**93–102.
18. **Lotscher, M., B. Kaissling, J. Bider, H. Murer, and M. Levi.** 1997. Role of microtubules in the rapid regulation of renal phosphate transport in response to acute alterations in dietary phosphate content. J. Clin. Investig. **99:**1302–1312.
19. **McClure, M. A., M. S. Johnson, D. F. Feng, and R. F. Doolittle.** 1988. Sequence comparisons of retroviral proteins: relative rate of change and general phylogeny. Proc. Natl. Acad. Sci. USA **85:**2469–2473.
20. **Miller, A. D.** 1996. Cell-surface receptors for retrovirus and implications for gene transfer. Proc. Natl. Acad. Sci. USA **93:**11407–11413.
21. **Murer, H., and J. Biber.** 1996. Molecular mechanisms of renal apical Na/phosphate cotransport. Annu. Rev. Physiol. **58:**607–618.
22. **Murer, H., I. Forster, M. Pfister, B. Kaissling, M. Lotscher, and J. Biber.** 1998. Cellular/molecular control of renal Na/Pi-cotransport. Kidney Int. **65:**S2–S10.
23. **Palmer, G., J. P. Boujour, and J. Caverzasio.** 1997. Expression of a newly identified phosphate transport/retrovirus receptor in human SaOS-2 osteoblast-like cells and its regulation by insulin-like growth factor I. Endocrinology **138:**5202–5209.
24. **Peerce, B. E.** 1995. Effect of substrates and pH on the intestinal Na+/phosphate cotransporter: evidence for an intervesicular divalent phosphate allosteric regulatory site. Biochim. Biophys. Acta **1239:**1–10.
25. **Peerce, B. E.** 1997. Interaction of substrates with the intestinal brush border membrane Na/phosphate cotransporter. Biochim. Biophys. Acta **1323:**45–56.
26. **Peerce, B. E., M. Cedilote, and R. D. Clarke.** 1995. Examination of the molecular mechanism of SH reagent-induced inhibition of the intestinal brush-border membrane Na/phosphate cotransporter. Biochim. Biophys. Acta **1239:**11–21.
27. **Pfister, M. F., H. Hilfiker, J. Forgo, E. Lederer, J. Biber, and H. Murer.** 1998. Cellular mechanisms involved in the acute adaptation of OK cell Na/Pi cotransport to high- or low-Pi medium. Pfluegers Arch. Eur. J. Physiol. **435:**713–719.
28. **Pfister, M. F., G. Stange, U. Ziegler, E. Lederer, J. Biber, and H. Murer.** 1998. Parathyroid hormone leads to the lysosomal degradation of the renal type II Na/Pi cotransporter. Proc. Natl. Acad. Sci. USA **95:**1909–1914.
29. **Pollock, A. S., and H. L. Santiesteban.** 1995. Calbindin expression in renal

tubular epithelial cells. Altered sodium phosphate co-transport in association with cytoskeletal rearrangement. J. Biol. Chem. **270:**16291–16301.
30. **Ragheb, J. A., H. Yu, T. Hofmann, and W. F. Anderson.** 1995. The amphotropic and ecotropic murine leukemia virus envelope TM subunits are equivalent mediators of direct membrane fusion: implications for the role of the ecotropic envelope and receptor in syncytium formation and viral entry. J. Virol. **69:**7205–7215.
31. **Saïb, A., F. Puvion-Dutilleul, M. Schmid, J. Périès, and H. de Thé.** 1997. Nuclear targeting of incoming human foamy virus Gag proteins involves a centriolar step. J. Virol. **71:**1155–1161.
32. **Thomsen, S., B. Vogt, D. von Laer, C. Heberlein, A. Rein, W. Ostertag, and C. Stocking.** 1998. Lack of functional PiT-1 and PiT-2 expression on hematopoietic stem cell lines. Acta Haematol. **99:**148–155.
33. **Van Zeijl, M., S. V. Johann, E. Closs, J. Cunningham, R. Eddy, T. B. Shows, and B. O'Hara.** 1994. A human amphotropic retrovirus receptor is a second member of the gibbon ape leukemia virus receptor family. Proc. Natl. Acad. Sci. USA **91:**1168–1172.
34. **Xiao, Y., C. J. Boyer, E. Vincent, A. Dugre, V. Vachon, M. Potier, and R. Béliveau.** 1997. Involvement of disulphide bonds in the renal sodium/phosphate co-transporter NaPi-2. Biochem. J. **323:**401–408.
35. **Yee, J. K., A. Miyanohara, P. LaPorte, K. Bouic, J. C. Burns, and T. Friedmann.** 1994. A general method for the generation of high-titer, pantropic retroviral vectors: highly efficient infection of primary hepatocytes. Proc. Natl. Acad. Sci. USA **91:**9564–9568.